PCCP

PAPER

View Article Online
View Journal | View Issue

Cite this: *Phys. Chem. Chem. Phys.*, 2016, **18**, 21481

From adsorption to condensation: the role of adsorbed molecular clusters

Sima Yaghoubian, Seyed Hadi Zandavi and C. A. Ward*

Received 22nd April 2016,
Accepted 5th July 2016

DOI: 10.1039/c6cp02713j

www.rsc.org/pccp

The adsorption of heptane vapour on a smooth silicon substrate with a lower temperature than the vapour is examined analytically and experimentally. An expression for the amount adsorbed under steady state conditions is derived from the molecular cluster model of the adsorbate that is similar to the one used to derive the equilibrium Zeta adsorption isotherm. The amount adsorbed in each of a series of steady experiments is measured using a UV-vis interferometer, and gives strong support to the amount predicted to be adsorbed. The cluster distribution is used to predict the subcooling temperature required for the adsorbed vapour to make a disorder–order phase transition to become an adsorbed liquid, and the subcooling temperature is found to be 2.7 ± 0.4 K. The continuum approach for predicting the thickness of the adsorbed liquid film originally developed by Nusselt is compared with that measured and is found to over-predict the thickness by three-orders of magnitude.

1 Introduction

Our objective is to develop a method for predicting the conditions under which film-wise condensation is initiated: *i.e.* the initiation of the transition from an adsorbed vapour to an adsorbed liquid when a stagnant vapour with temperature, T^{V}, is exposed to a planar, vertically oriented, smooth substrate with a lower temperature, T^{S}. We examine the predictions using heptane adsorbing on silicon, and measure, at one position on the disk, the adsorbed film thickness using a UV-vis interferometer.

If the saturation temperature corresponding to the vapour-phase pressure, P^{V}, is denoted $T_{sat}(P^{V})$, the continuum approach to predicting the thickness of an adsorbed liquid film assumes that a liquid film forms whenever ΔT:

$$\Delta T \equiv [T_{sat}(P^{V}) - T^{S}], \quad (1)$$

is greater than zero,[1,2] *i.e.* without subcooling. Our experiments do not support this assumption. Compared to the measurements, the continuum approach is found to strongly over-predict the liquid film thickness.

When a vapour at T^{V} is exposed to a cooler substrate, we suppose that the adsorbate can be approximated as a collection of molecular clusters, similar to that assumed to develop the equilibrium Zeta adsorption isotherm.[3] In both cases, the number of clusters of type ζ in the adsorbate is denoted $a_{\zeta}(y^{VS})$, where ζ is the number of molecules in a cluster, and the temperature function, y^{VS}, is defined as

$$y^{VS} \equiv [P^{V}/P_{sat}(T^{S})]^{T^{V}/T^{S}}. \quad (2)$$

ζ has a maximum value of ζ_{m}, but it is allowed values to have of 1, 2, 3,…ζ_{m}. We develop an expression for the cluster distribution $a_{\zeta}(y^{VS})$ in steady, thermal disequilibrium states that have an interfacial temperature discontinuity at the solid–vapour interface.[4–6] From $a_{\zeta}(y^{VS})$, we obtain the expression for the amount adsorbed in the thermal disequilibrium, $\eta_{td}(y^{VS})$.

The interfacial temperature discontinuity indicates that even though the system is in a steady state under the system constraints, there is condensation occurring on certain cluster-types, but simultaneously, others are evaporating. This has the net result that at a value of y^{VS}, the thickness of the adsorbate is in the steady state. This hypothesis is supported by the experimental observations.

In our experiments, a smooth silicon disk maintained at a series of progressively lower temperatures, T^{S}, is exposed to heptane vapour saturated at 301 ± 0.2 K. The entropy of the adsorbate increases until a state of maximum disorder is reached. Then a disorder–order phase transition[7] is initiated that converts the adsorbed vapour to a heterogeneous phase of adsorbed liquid and adsorbed vapour. As T^{S} is lowered further, the entropy of the surface phase decreases, indicating that the adsorbed phase becomes more ordered as it is converted into an adsorbed liquid phase.

1.1 Basis for predicting the amount adsorbed in steady, thermal disequilibrium states

We suppose, firstly that a necessary condition for the system considered to be a thermal disequilibrium, steady state is that

Thermodynamics and Kinetics Laboratory, Department of Mechanical and Industrial Engineering, University of Toronto, 5 King's College Road, Toronto, Canada M5S 3G8. E-mail: charles.ward@utotonto.ca; Fax: +1-416-978-7753

the chemical potential of the molecules in the vapour phase, μ^{V}, should have the same value as that of the single-molecule adsorbed "clusters", μ_1^{SV}, on the solid surface at temperature T^{S}:

$$\mu_1^{SV}(T^{S}) = \mu^{V}(T^{V}). \quad (3)$$

Only clusters with one molecule are allowed to be exchanged with the vapour phase. Note that even though the chemical potentials of the molecules in the two phases are equal, there can be molecular transport between the phases, since the temperatures of the phases are different.

Secondly, we suppose that the adsorbed vapour is in local thermodynamic equilibrium at T^{S}, and consists of a cluster distribution that forms as a result of reactions on the surface between single-adsorbed molecules, A_1, and adsorbed, multiple-molecule clusters A_2, A_3,.. A_{ζ_m}. Symbolically then, the surface reactions may be expressed as:

$$\begin{aligned} A_1 + A_1 &\rightleftharpoons A_2, \\ A_1 + A_2 &\rightleftharpoons A_3, \\ &\vdots \\ A_1 + A_{\zeta_m - 1} &\rightleftharpoons A_{\zeta_m}. \end{aligned} \quad (4)$$

For this adsorbed phase to be in local equilibrium:

$$\begin{aligned} \mu_1^{SV} + \mu_1^{SV} &= \mu_2^{SV}, \\ \mu_1^{SV} + \mu_2^{SV} &= \mu_3^{SV}, \\ &\vdots \\ \mu_1^{SV} + \mu_{\zeta_m - 1}^{SV} &= \mu_{\zeta_m}^{SV}, \end{aligned} \quad (5)$$

or, simply

$$\mu_\zeta^{SV}(T^{S}) = \zeta \mu_1^{SV}(T^{S}), \quad \zeta = 1, 2, \ldots \zeta_m. \quad (6)$$

Thus, the surface phase is approximated as homogeneous with possibly ζ_m cluster-types present, but the chemical potential per molecule is uniform in the surface phase.[3,8] We use eqn (3) and (6) as the basis for developing an analytical expression for the cluster distribution a_ζ, and then use a_ζ to develop the expression for the amount adsorbed under both equilibrium and thermal disequilibrium conditions, $\eta_{td}(y^{VS})$.

We emphasize that the thermal equilibrium version of eqn (3) and (6) was the basis for the derivation of the equilibrium Zeta adsorption isotherm, $n^{SV}(x^{V})$, where x^{V} is the pressure ratio, $P^{V}/P_{sat}(T)$.[3] As will be seen, under thermal disequilibrium conditions, $\eta_{td}(y^{VS})$ describes the amount adsorbed, but $\eta_{td}(y^{VS})$ automatically reduces to the Zeta adsorption isotherm when thermal equilibrium exists in the system, and this isotherm has significant experimental support.[3,9–15]

In the thermal disequilibrium steady states considered, we measure the thickness of the adsorbed liquid film using a UV-vis interferometer, compare that measured with that predicted using the continuum model,[1] and find that the continuum prediction is three-orders of magnitude larger than the experimental value. In addition to the assumption of no subcooling required to initiate the liquid phase, the continuum approach uses the heat transfer coefficient approximation, and assumes that the thickness of the adsorbed layer is determined by thermal conduction across the adsorbed layer. As discussed in Section 6, in the approach we propose that there is no need to introduce the heat transfer coefficient approximation.

2 Experimental apparatus and measurements

The experimental apparatus shown schematically in Fig. 1 was designed to measure the thickness of the heptane adsorbate at one position on a vertically oriented Si disk as a function of y^{VS}. Inside the stainless-steel chamber, the Si disk was mounted at one end of a stainless steel cylinder that transported the cooling fluid to maintain the disk at T^{S}. One side of the disk was polished and could be viewed through a quartz window (Kurt J. Lesker, USA) using the light source of the UV-visible interferometer (Filmetrics, USA). The interferometer light source was focused at a point 14.4 mm above the bottom of the Si disk (Fig. 1). The Si disk (Sil'tronix S.T., Fr) had a 18 mm diameter, a thickness of 10 mm, and a central hole of 1 mm-Dia. The disk surface had been polished using a chemical, mechanical polishing process that the manufacturer claimed provided a surface roughness of less than 1 nm.

A total of twelve thermocouples (TCs) had been implanted in the 10 mm thickness of the disk; four at each of three longitudinal depths.[5] At each of these depths, the thermocouples were placed at radial depths of 1.0, 3.0, 5.0, and 7.0 mm, measured from the centreline, and were separated by 90° around the disk circumference. These thermocouples were used to determine the interfacial solid temperature, T^{S}, during each experiment.

For cleanliness, the stainless steel chamber was evacuated using a stainless-steel turbo-molecular diffusion pump to a pressure of 10^{-6} Pa and held under this condition for over 48 hours. With the light source of the UV-visible interferometer at the position to be used subsequently, the baseline spectrum of the Si surface was recorded before the heptane was admitted to the chamber. It was found to be the standard spectrum of Si in the absence of adsorption.[16,17]

A sample of the gas–vapour mixture in the chamber was drawn into a residual gas analyzer (SRS Model RGA 200) both before and after each experiment. The gas remaining in the chamber before an experiment was primarily N_2 at a partial pressure of 10^{-6} Pa. After an experiment, only heptane was detected.

The heptane that was to be introduced into the chamber was first degassed in the flask outside the chamber, as shown schematically in Fig. 1. At the end of the degassing process, the vapour-phase pressure and the temperature in the flask were measured. The vapour-phase pressure corresponded to the saturation–vapour pressure at the measured temperature, indicating that the heptane was degassed. Afterwards, the heptane was transferred from the degassing flask to the

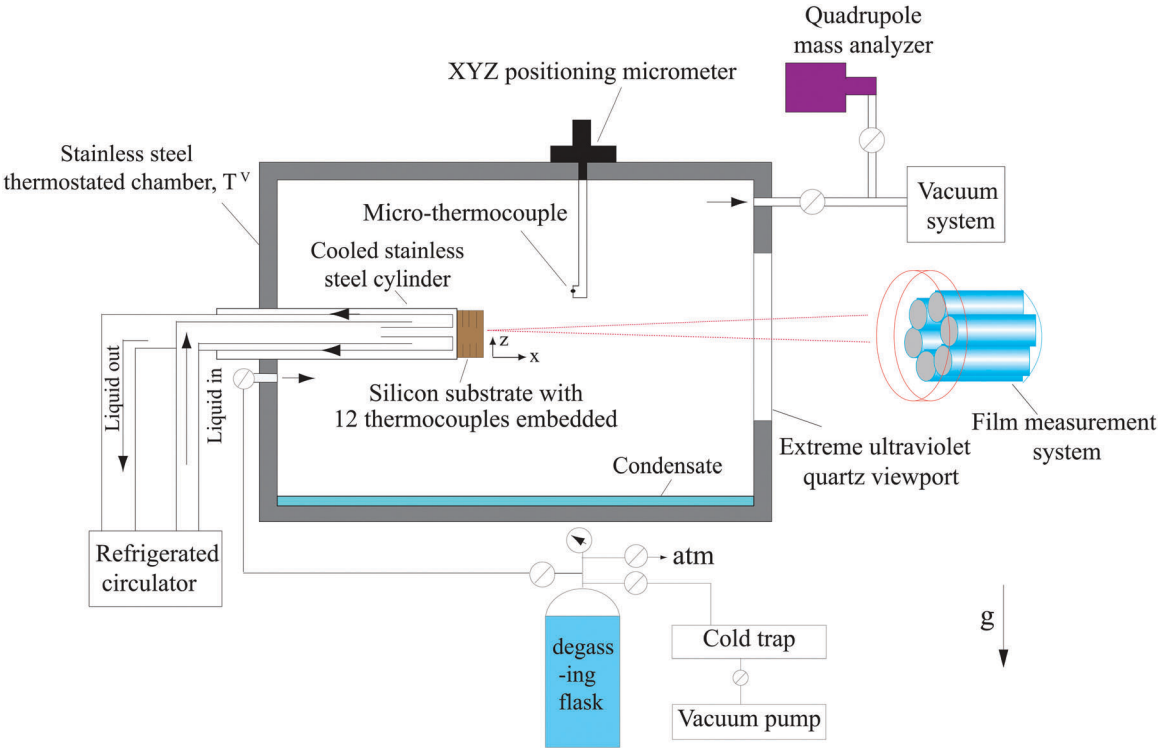

Fig. 1 A schematic of the experimental chamber and the associated equipment is shown. The experiments were conducted in three steps: (1) the chamber was evacuated using a stainless steel ultra high vacuum system to 10^{-6} and held under this condition for 48 hours. Under this condition, the UV-vis interferometer system was used to scan the silicon substrate. (2) The heptane vapour was admitted to the chamber and the chamber walls were maintained at 301 K. The stainless cylinder inside the chamber and the Si substrate was cooled to a series of temperatures, T^S. The substrate surface temperature was established from measurements with 12 thermocouples implanted in the substrate. (3) Once the system had reached the steady state, the interferometer was used to measure the thickness of the adsorbate. The measurements at each of the y^{VS} values are summarized in Table 1.

chamber without exposure to the atmosphere using the vacuum system indicated in Fig. 1. With the heptane flowing slowly through the chamber, the cooling of the solid substrate to T^S was initiated. It was maintained constant during each experiment and ranged from 298.8 ± 0.1 K down to 295.7 ± 0.1 K in the different experiments. Using an independent cooling circuit, the chamber walls were maintained at 301 ± 0.2 K. The criterion for the steady-state was that the system temperatures did not change by more than 1% in 30 minutes.

During the period required to bring the system to the steady state (approximately three hours), we assume that some heptane condensed on the "cooled stainless steel cylinder" resulting in a shallow condensate pool, as indicated schematically in Fig. 1. When the system had reached the steady state, the temperature near the chamber walls, T^V, was measured using a calibrated micro-thermocouple (±0.05 K) that had a bead diameter of 25 μm, and was mounted on a positioning micrometer. Thus, in the thermal disequilibrium steady states, we take the pressure in the chamber, P^V, to be $P_{sat}(T^V)$, and the temperature function then becomes

$$y^{VS} = \left[\frac{P_{sat}(T^V)}{P_{sat}(T^S)}\right]^{T^V/T^S} \quad (7)$$

The readings of the twelve thermocouples were recorded, and subsequently used to determine the T^S for each experiment.

Once the system had reached the steady state, a second spectrum was recorded using the interferometer, and the two interferometer spectra of the Si surface were used with the software provided by the manufacturer to determine the thickness of the adsorbed film, τ_m, for each value of y^{VS}. All of the experimental results are listed in Table 1. The measured values of τ_m are also shown in Fig. 2. Note that as y^{VS} was increased from 1.12 to approximately 1.22, τ_m reached its plateau value.

3 Steady state cluster distributions

In each of the experiments, the system was observed to evolve to a steady state at a given value of y^{VS}. We assume that this state is reached when the two conditions listed in eqn (3) and (6) are reached, and that the vapour phase may be approximated as an ideal gas. We first show that the chemical potential of the saturated vapour, $\mu[T^V, P_{sat}(T^V)]$, may be expressed in terms of y^{VS} and the chemical potential was evaluated at T^V and $P_{sat}(T^S)$.

The ideal gas chemical potential, $\mu^V(T, P)$, may be written as

$$\mu^V(T,P) = f(T) + k_B T \ln P, \quad (8)$$

where $f(T)$ is an arbitrary function of temperature. We evaluate it by applying the relation at T^V and $P_{sat}(T^V)$:

$$f(T^V) = \mu^V[T^V, P_{sat}(T^V)] - k_B T^V \ln P_{sat}(T^V). \quad (9)$$

Table 1 Measured thicknesses of heptane films adsorbed on silicon, $\tau_m(y^{VS})$ for T^V = 301 ± 0.2

y^{VS}	T^V (K)	$P_{sat}(T^V)$ (Pa)	T^S (K)	$P_{sat}(T^S)$ (Pa)	τ_m (nm)	ΔT (K)	δ_c (μm)	v_f (m^3 kmol^{-1})	$\frac{\tau_m}{v_f}$(μmol m^{-2})	$\eta_{td}(y^{VS})$ (μmol m^{-2})
1.12	301.1	7044	298.8	6291	28	2.3	31.8	0.1476	190	134
±0.01	±0.1	±34	±0.1	±34	±21%	±0.2		0.0001		±54%
1.13	301.2	7078	298.7	6260	49	2.5	32.5	0.1476	332	235
±0.01	±0.1	±34	±0.1	±34	±16%	±0.2		0.0001		±60%
1.15	301.2	7078	298.4	6167	77	2.8	33.5	0.1475	522	586
±0.01	±0.1	±34	±0.1	±34	±10%	±0.2		0.0001		±21%
1.17	301.2	7078	298.0	6045	99	3.2	34.7	0.1474	672	709
±0.01	±0.1	±34	±0.1	±34	±9%	±0.2		0.0001		±4%
1.22	301.0	7010	297.1	5779	112	3.9	36.5	0.1473	760	760
±0.01	±0.1	±34	±0.1	±34	±6%	±0.2		0.0001		±1%
1.23	301.2	7078	297.0	5750	114	4.2	37.2	0.1473	774	764
±0.01	±0.1	±34	±0.1	±34	±6%	±0.2		0.0001		±1%
1.28	300.9	6976	296.0	5466	117	4.9	38.8	0.1471	795	774
±0.01	±0.1	±34	±0.1	±34	±4%	±0.2		0.0001		±1%
1.29	300.9	6976	295.8	5411	118	5.1	39.2	0.1470	803	775
±0.01	±0.1	±34	±0.1	±34	±4%	±0.2		0.0001		±1%
1.31	301.0	7010	295.7	5384	117	5.3	39.4	0.1470	796	777
±0.01	±0.1	±34	±0.1	±34	±4%	±0.2		0.0001		±1%

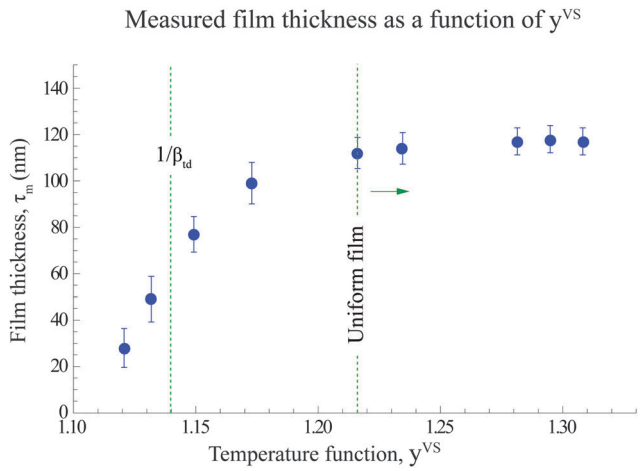

Fig. 2 The measured thicknesses of the adsorbate as a function of y^{VS} are depicted. The error bars indicate the error determined from at least ten repeated measurements using the software of the manufacturer. The explicit error bars in the values of τ_m are listed in Table 1.

After replacing $f(T^V)$ in eqn (8), one finds

$$\mu^V(T^V, P) = \mu^V[T^V, P_{sat}(T^V)] + k_B T^V \ln\left(\frac{P}{P_{sat}(T^V)}\right), \quad (10)$$

where P is an arbitrary pressure. We apply the relation at P equal to $P_{sat}(T^S)$, and solve for $\mu^V[T^V, P_{sat}(T^V)]$:

$$\mu^V[T^V, P_{sat}(T^S)] = \mu^V[T^V, P_{sat}(T^V)] + k_B T^V \ln\left[\frac{P_{sat}(T^S)}{P_{sat}(T^V)}\right]. \quad (11)$$

Since the temperature function, y^{VS}, for the experiments is given in eqn (7), we may obtain from eqn (11) the expression for $\mu^V[T^V, P_{sat}(T^V)]$ in terms of y^{VS}

$$\mu^V[T^V, P_{sat}(T^V)] = k_B T^V \ln\left\{(y^{VS})^{(T^S/T^V)} \exp\left[\frac{\mu^V[T^V, P_{sat}(T^S)]}{k_B T^V}\right]\right\}. \quad (12)$$

This relation reduces to an identity when thermal equilibrium exists in the system.

The expression for μ_1^{SV} of the adsorbed phase was constructed by Ward and Wu.[3] They approximated each degree of freedom of an adsorbed cluster as a quantum mechanical, harmonic oscillator that had a fundamental frequency depending on the number of molecules in the cluster, $\omega^{(\zeta)}$. We follow their procedure. The possible energy levels of a degree of freedom are

$$\varepsilon_k^{(\zeta)} = \varepsilon_0^{(\zeta)} + k\hbar\omega^{(\zeta)}; \quad \zeta = 1, 2, 3\ldots\zeta_m; \quad k = 0, 1, 2, 3\ldots, \quad (13)$$

where $\varepsilon_0^{(\zeta)}$ is the zero point energy of each degree of freedom of a cluster of ζ molecules, and $\hbar$ denotes the Planck constant divided by 2π. The canonical ensemble and statistical thermodynamics were then applied to obtain the chemical potential expression of a cluster with ζ molecules:

$$\mu_\zeta^{SV} = k_B T^S \ln\left(\frac{a_\zeta}{a_0 q_\zeta}\right), \quad (14)$$

where a_0 is the number of empty adsorption sites, and q_ζ is the partition function of a cluster with ζ molecules, and may be written as

$$q_\zeta = \left(\frac{\exp\left[\frac{-\varepsilon_0^{(\zeta)}}{k_B T^S}\right]}{1 - \exp\left[\frac{-\hbar\omega^{(\zeta)}}{k_B T^S}\right]}\right)^3. \quad (15)$$

For comparison with the equilibrium Zeta adsorption isotherm,[3] we use the same parameterization and introduce, q_v

$$q_\zeta = q_1(q_v)^{\zeta-1}, \quad \zeta = 1, 2, 3\ldots\zeta_m. \quad (16)$$

With this parameterization, eqn (14) and (16) give

$$a_\zeta = a_0 q_1 (q_v)^{\zeta-1} \exp\left(\frac{\mu_\zeta^{SV}}{k_B T^S}\right); \quad (17)$$

thus, for ζ equal to unity, eqn (17) gives

$$a_1 = a_0 q_1 \exp\left(\frac{\mu_1^{SV}}{k_B T^S}\right),$$

or

$$a_1 = a_0 q_1 \left[\exp\left(\frac{\mu_1^{SV}}{k_B T^V}\right)\right]^{\frac{T^V}{T^S}}. \quad (18)$$

From eqn (3), (12) and (18), one finds

$$a_1 = a_0 q_1 y^{VS} \left\{\exp\frac{\mu^V\left[T^V, P_{sat}\left(T^S\right)\right]}{k_B T^V}\right\}^{\frac{T^V}{T^S}} \quad (19)$$

Recall that a_1 is the number of adsorbed clusters that consist of one molecule, and eqn (19) results from the condition for the steady state between the vapour phase at T^V and the adsorbed phase at T^S, eqn (3) and (14).

When eqn (6) is combined with eqn (3), the chemical potential of a cluster with ζ molecules can be written as

$$\mu_\zeta^{SV}(T^S) = \zeta\mu^V(T^V), \quad (20)$$

after making use of eqn (12), $\mu_\zeta^{SV}(T^S)$ may be written as

$$\mu_\zeta^{SV}\left(T^S\right) = \zeta\left\{k_B T^V \ln\left[\left(y^{VS}\right)^{\left(T^S/T^V\right)}\exp\left[\frac{\mu^V\left[T^V, P_{sat}\left(T^S\right)\right]}{k_B T^V}\right]\right]\right\} \quad (21)$$

when eqn (21) is substituted in eqn (17), the result can be written as

$$a_\zeta = a_0 q_1 (q_v)^{\zeta-1}\left\{\exp\left[\ln\left(\left(y^{VS}\right)^\zeta\right)\left(\frac{\mu^V\left(T^V, P_{sat}\left(T^S\right)\right)}{k_B T^V}\right)^{\zeta\frac{T^V}{T^S}}\right]\right\}, \quad (22)$$

it may be simplified to:

$$a_\zeta = a_0 q_1 (q_v)^{\zeta-1}\left(y^{VS}\right)^\zeta\left(\exp\frac{\mu\left(T^V, P_{sat}\left(T^S\right)\right)}{k_B T^V}\right)^{\zeta\frac{T^V}{T^S}}, \quad (23)$$

and, from eqn (19) and (23), one finds

$$a_\zeta = a_1\left(q_v y^{VS}\right)^{(\zeta-1)}\left\{\exp\frac{\mu\left[T^V, P_{sat}\left(T^S\right)\right]}{k_B T^V}\right\}^{(\zeta-1)\frac{T^V}{T^S}}. \quad (24)$$

This equation relates a_ζ to conditions in the vapour phase. Even though clusters with more than one molecule are not exchanged with the vapour phase, the relation comes because A_1 is in local equilibrium with the other adsorbed clusters, A_ζ, and with the vapour phase as required by eqn (3) and (6).

3.1 Expression for the amount adsorbed in steady, thermal disequilibrium states

Since the number of clusters that have ζ molecules is denoted a_ζ, the total number of molecules adsorbed in the steady thermal-disequilibrium states, $\eta_{td}(y^{VS})$, may be expressed as

$$\eta_{td}\left(y^{VS}\right) = \sum_{\zeta=1}^{\zeta_m}\zeta a_\zeta\left(y^{VS}\right). \quad (25)$$

The expression we have established for a_ζ depends on a_0, eqn (17). We use the total number of adsorption sites, M, and the number of occupied sites, n_{oc}, to establish a relation that a_0 must satisfy.

$$M = a_0 + n_{oc}, \quad (26)$$

and n_{oc} may be written as

$$n_{oc} = \sum_{\zeta=1}^{\zeta_m} a_\zeta; \quad (27)$$

thus,

$$\frac{a_0}{M} + \sum_{\zeta=1}^{\zeta_m}\frac{a_\zeta}{M} = 1. \quad (28)$$

combining eqn (23) and (28) one finds, after summing the finite series that

$$\frac{a_0}{M} = \frac{-1 + q_v\exp\left(\frac{\mu^V\left(T^V, P_{sat}\left(T^S\right)\right)}{k_B T^S}\right)y^{VS}}{g} \quad (29)$$

where

$$\begin{aligned} g \equiv\ & -1 + q_v\exp\left(\frac{\mu^V\left(T^V, P_{sat}\left(T^S\right)\right)}{k_B T^S}\right)y^{VS} \\ & - q_1\exp\left(\frac{\mu^V\left(T^V, P_{sat}\left(T^S\right)\right)}{k_B T^S}\right)y^{VS} \\ & + q_1(q_v)^{\zeta_m}\left\{\exp\left(\frac{\mu^V\left(T^V, P_{sat}\left(T^S\right)\right)}{k_B T^S}\right)y^{VS}\right\}^{(1+\zeta_m)} \end{aligned} \quad (30)$$

introduces two thermal-disequilibrium parameters β_{td} and c_{td}:

$$\beta_{td}\left(T^V, T^S\right) \equiv q_v\left(T^S\right)\exp\left(\frac{\mu^V\left(T^V, P_{sat}\left(T^S\right)\right)}{k_B T^S}\right), \quad (31)$$

and

$$c_{td}\left(T^S\right) \equiv \frac{q_1\left(T^S\right)}{q_v\left(T^S\right)}, \quad (32)$$

then, a_0/M can be written as

$$\frac{a_0}{M} = \frac{-1 + \beta_{td}y^{VS}}{-1 + \beta_{td}y^{VS} - c_{td}\beta_{td}y^{VS} + c_{td}\left(\beta_{td}y^{VS}\right)^{(1+\zeta_m)}}. \quad (33)$$

After substituting eqn (33) into eqn (23), one finds

$$\frac{a_\zeta}{M} = \frac{c_{td}\left(\beta_{td}y^{VS} - 1\right)\left(\beta_{td}y^{VS}\right)^\zeta}{\beta_{td}y^{VS}\left(1 + c_{td}\left(\left(\beta_{td}y^{VS}\right)^{\zeta_m} - 1\right)\right) - 1}, \quad \zeta = 1,\ 2, \ldots, \zeta_m. \quad (34)$$

The expression for a_ζ, given in eqn (34), may be inserted into eqn (25), and the result was summed to obtain the expression

for η_{td}:

$$\eta_{td}(y^{VS}) = \frac{Mc_{td}\beta_{td}y^{VS}\left[1-(1+\zeta_m)(\beta_{td}y^{VS})^{\zeta_m}+\zeta_m(\beta_{td}y^{VS})^{1+\zeta_m}\right]}{(1-\beta_{td}y^{VS})\left[1+(c_{td}-1)\beta_{td}y^{VS}-c_{td}(\beta_{td}y^{VS})^{1+\zeta_m}\right]}. \quad (35)$$

In order to apply the expression for $\eta_{td}(y^{VS})$ given in eqn (35), we must determine the values of M, c_{td}, ζ_m and β_{td}. Below we will use equilibrium adsorption measurements for this purpose. But we note that the fundamental assumptions made in eqn (3) and (6) are the ones used to obtain the results listed in eqn (33) to (35).

3.2 The limits of $\beta_{td}y^{VS}$ approaching unity

When the expression for the cluster distribution, a_ζ, given in eqn (34), and the expression for $\eta_{td}(y^{VS})$ given in eqn (35) are examined in the limit of $\beta_{td}y^{VS}$ approaching unity, the result indicates the singularities of the zero-over-zero type in both relations. But if the l'Hôpital rule is applied to each, one finds

$$\lim_{(\beta_{td}y^{VS}\to 1)} a_\zeta(y^{VS}) = \frac{Mc_{td}}{1+c_{td}\zeta_m}, \quad (36)$$

and

$$\lim_{(\beta_{td}y^{VS}\to 1)} \eta_{td}(y^{VS}) = \frac{Mc_{td}\zeta_m(1+\zeta_m)}{2(1+c_{td}\zeta_m)}. \quad (37)$$

Since c_{td} and ζ_m are finite, there are no actual singularities in either function.

As will be seen, the steady state corresponding to y^{VS} equal to ${\beta_{td}}^{-1}$ is the state where the phase transition is predicted to be initiated. These relations, eqn (36) and (37), will aid in showing that the transition is a disorder–order type transition.

4 Equilibrium adsorption of heptane on a silicon nanopowder

In the equilibrium adsorption limit, T^S and T^V have the same value, denoted T, and P^V is less than the saturation vapour pressure corresponding to this temperature, $P_{sat}(T)$. In this limit, y^{VS}, eqn (2) goes to

$$\lim_{[T^S,T^V\to T, P^V<P_{sat}(T)]} y^{VS} \to x^V,$$

where

$$x^V \equiv P^V/P_{sat}(T), \quad \text{and } x^V < 1. \quad (38)$$

β_{td} becomes:

$$\lim_{(T^S,T^V\to T),\ P^V<P_{sat}(T)} \beta_{td}(T^V,T^S) = q_v(T)\exp\left(\frac{\mu^V(T,P_{sat}(T))}{k_BT}\right), \equiv \alpha(T). \quad (39)$$

$c_{td}(T^S)$ reduces to

$$\lim_{(T^S,T^V\to T)} c_{td}(T^S) = \frac{q_l(T)}{q_v(T)} \equiv c(T). \quad (40)$$

Finally, in view of eqn (38) to (40), in this limit $\eta_{td}(y^{VS})$, eqn (35), becomes $n^{SV}(x^V)$, the amount adsorbed under equilibrium conditions, according to the equilibrium Zeta adsorption isotherm:

$$\lim_{(T^S,T^V\to T),P^V<P_{sat}(T)} \eta_{td}(y^{VS}) = n^{SV}(x^V)$$

where

$$n^{SV}(x^V) = \frac{Mc\alpha x^V\left[1-(1+\zeta_m)(\alpha x^V)^{\zeta_m}+\zeta_m(\alpha x^V)^{1+\zeta_m}\right]}{(1-\alpha x^V)\left[1+(c-1)\alpha x^V-c(\alpha x^V)^{1+\zeta_m}\right]}. \quad (41)$$

Thus, in the equilibrium adsorption limit, $\eta_{td}(y^{VS})$ reduces to the equilibrium Zeta adsorption isotherm and it contains the four isotherm constants: M, c, α and ζ_m.

4.1 Measured equilibrium adsorption of heptane on a silicon nanopowder

We now propose to use equilibrium adsorption measurements and determine the values of the Zeta adsorption isotherm constants for heptane adsorbing silicon.[12–15] In eqn (41), n^{SV} is the amount adsorbed per unit area. It may convert the amount adsorbed per unit mass of the substrate by replacing M with

$$M = \frac{M_g}{A_{sat}(Si)}. \quad (42)$$

where M_g is the number of adsorption sites per unit mass of the adsorbent, and $A_{sat}(Si)$ is the specific surface area, and can be expressed as

$$A_{sat}(Si) = M_g\bar{\sigma}_{heptane}, \quad (43)$$

Table 2 Equilibrium Zeta adsorption isotherm constants at 301 K, and thermal disequilibrium parameters for heptane adsorbing on silicon

Equilibrium	M_g (μmol mg^{-1})	$\bar{\sigma}_{heptane}$ (Å)^2	M (μmol m^{-2})	c	α	ζ_{th}
$0 < x^V < 0.95$	0.048 ±0.002	73 ±3	2.27 ±0.1	8.5 ±1.2	0.875 ±0.005	100
Thermal dis-equilibrium	M_g (μmol mg^{-1})	$\bar{\sigma}_{heptane}$ (Å)^2	M (μmol m^{-2})	$c_{td}(T^S)$	$\beta_{td}(T^V,T^S)$	ζ_m
$1 < y^{VS} < 1.31$	0.048 ±0.002	73 ±3	2.27 ±0.1	8.5 ±1.2	0.875 ±0.005	356

where $\bar{\sigma}_{heptane}$ is the average cross-sectional area of an adsorption site. Its value was determined by Zandavi and Ward,[13] and is listed in Table 2.

The value of ζ_m cannot be determined from the equilibrium adsorption measurements. Only the threshold value, ζ_{th}, can be obtained from such measurements. As demonstrated by Ward and Wu,[3] when a value of ζ_m is assumed that is less than ζ_{th}, the agreement between the calculated equilibrium adsorption compared to that measured increases as the assumed value of ζ_m is increased, until ζ_{th} is reached. If the assumed value of ζ_m is increased above ζ_{th}, the agreement does not increase further. We shall determine ζ_m from the adsorbed-film thickness measurements, Fig. 2. Provided the value of ζ_m is greater than the ζ_{th}, the amount calculated to be adsorbed under equilibrium conditions will not be affected by replacing ζ_{th} with ζ_m. We use the equilibrium gravimetric measurements of the adsorption and desorption isotherms of heptane vapour adsorbing on a silicon nanopowder (Sigma Aldrich) to determine the value of the equilibrium adsorption isotherm parameters. The measurement procedure used is similar to that described previously:[12–15] a sample of approximately 10 mg of the silicon nanopowder was placed in an adsorption apparatus (Surface Measurements Systems) and heated in a N_2 atmosphere to 423 K, and held at this temperature for four hours. After cooling to 301 K, gravimetric measurements were made with n_g^{SV} when anhydrous, *n*-heptane (Sigma Aldrich, 99% purity) was exposed to the nanopowder sample with x^V in the range of $0 < x^V \leq 0.95$. When the change in n_g^{SV} was less than 0.02% in 20 minutes at a value of x^V, the system was assumed to have reached equilibrium at that value of x^V.

The gravimetric measurements were converted to per unit area using $A_{sat}(Si)$. The amount adsorbed per unit area as a function of y^{VS} (or x^V) is shown in Fig. 3. The Nonlinear Regression Package of Mathematica™ was used to determine the values of the equilibrium adsorption isotherm parameters that are listed in Table 2. The calculated amount adsorbed using eqn (41) and the equilibrium isotherm parameters are shown as the solid line in Fig. 3. Note then for these experiments $y^{VS} \rightarrow x^V < 1$, eqn (38).

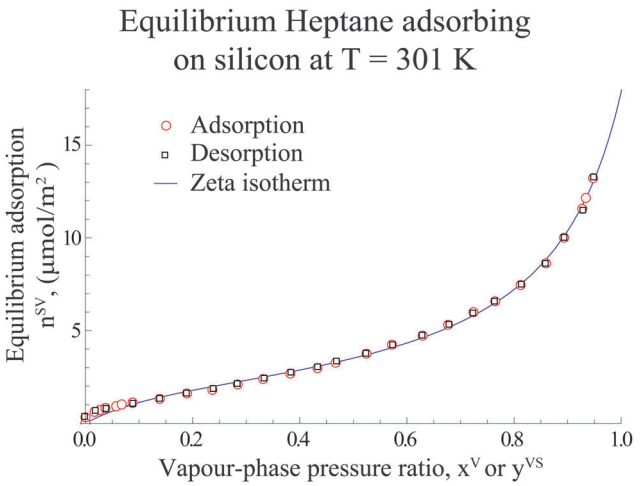

Fig. 3 The amount of heptane adsorbing-on and desorbing-from a Si nanopowder is shown. Note that the measurements are reversible. The data points were used with eqn (41) to determine the values of *M*, *c*, α, and ζ_{th} that are listed in Table 2. The error bars are within the symbols, indicating that the quality of the fit was very good.

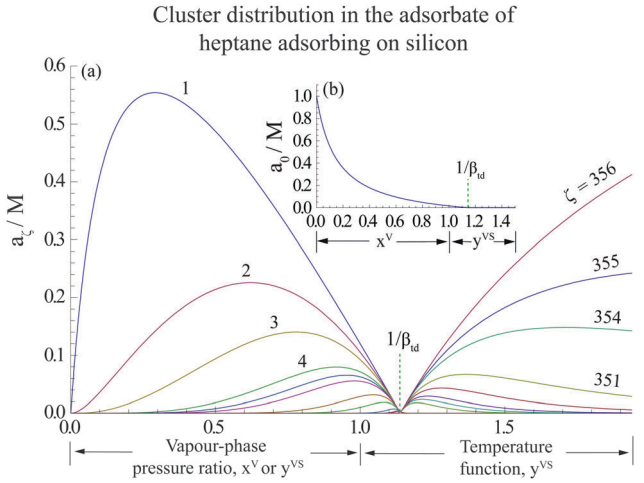

Fig. 4 For heptane vapour adsorbing on silicon: the calculated cluster distribution for ζ greater than or equal to unity as a function of the temperature function y^{VS} is depicted in (a). In (b) the calculated number of unoccupied sites, a_0, as a function of y^{VS} is indicated. As y^{VS} reaches $1/\beta_{td}$ the number of unoccupied sites approaches zero; the number of clusters reaches maximum: ζ_m; and each cluster-type has the same concentration in the adsorbate: from eqn (36) and the parameters listed in Table 2, one finds that a_ζ/M is 0.0028. As seen in Fig. 6, the entropy per molecule of the adsorbate is a maximum when this condition is reached.

For the thermal disequilibrium experiments shown in Fig. 4, both y^{VS} and T^V/T^S are each greater than or equal to unity, but we neglect any effect of reducing T^S below T^V on the value of the isotherm parameters, as indicated in Table 2. This assumption will be examined further when $\eta_{td}(y^{VS})$ is calculated using the thermal disequilibrium values of the parameters and compared with the measurements in Fig. 4.

5 The cluster distribution and the entropy of the adsorbate

As indicated in Section 4.1, the data shown in Fig. 3 were used with eqn (41) to determine constants appearing in Table 2 for $0 < x^V < 0.95$, and then we used the results found from the thermal equilibrium limits (eqn (39) and (40)) to justify the values of $c_{td}(T^S)$ and $\beta_{td}(T^V,T^S)$ listed in this table.

For y^{VS} equal to or greater than 1.22, as seen in Fig. 2, the measured film thickness, τ_m, was uniform. We assume that in the uniform range, the specific volume of the adsorbed fluid may be approximated as that of saturated liquid heptane, v_f, at the measured solid interface temperature, T^S. The adsorption in this range calculated on this basis is listed in the penultimate column of Table 1. Since the parameters, other than ζ_m, that appear in the expression for $\eta_{td}(y^{VS})$ have been determined, and are listed in Table 2, the Nonlinear Regression Package of

Mathematica™ may be used with eqn (35) and the measured amount adsorbed, $\tau_m/\nu_f(T^S)$, to determine the value of ζ_m that minimizes the difference between that measured and that predicted in the uniform range. The value of the ζ_m determined by this procedure is listed in Table 2. Note that the value of ζ_m is greater than the ζ_{th}.

5.1 The molecular cluster distribution indicates a phase transition

From eqn (33) and (34) and the parameters listed in Table 2, the cluster distributions $a_0(y^{VS})/M$ and $a_\zeta(y^{VS})/M$ as a function of y^{VS} were calculated and are shown in Fig. 4(a) and (b). For y^{VS} much less than $\beta_{td}{}^{-1}$, the adsorption sites are mostly empty; but when y^{VS} is increased to 0.13, the number of occupied sites exceeds the number of unoccupied sites. For y^{VS} approaching $\beta_{td}{}^{-1}$, the sites are mostly occupied by single molecules, and the clusters with ζ_m molecules occupy the smallest number of sites, but when y^{VS} reaches $\beta_{td}{}^{-1}$, as indicated by eqn (36) and Fig. 5, the number of each cluster-type in the adsorbate is the same. Since each cluster type would be identifiable, this means that the configuration degeneracy of the adsorbate—*i.e.* the number of ways the cluster-types could be distributed over the M adsorption sites—would be a maximum, as would be the disorder of the adsorbate.[3,7]

When y^{VS} exceeds $\beta_{td}{}^{-1}$, clusters with the largest number of molecules, ζ_m, become the dominate cluster-type in the adsorbate. We assume that these clusters are liquid-like and that when y^{VS} exceeds $\beta_{td}{}^{-1}$, the adsorbed liquid phase is initiated.

This assumption is supported by the measured amount adsorbed under both thermal equilibrium and disequilibrium conditions. The measured amount adsorbed for y^{VS} less than or equal to unity is shown on different scales in Fig. 3 and 4. For y^{VS} greater than or equal to unity, $\tau_m(y^{VS})/\nu_f$ is listed in Table 1 and shown as data points with error bars in Fig. 5. The calculated amount adsorbed obtained from eqn (35) using the parameters listed in Table 2 is shown in Fig. 5 as the solid line. Note that the calculated adsorption is within error bars of that measured.

The notion that a phase transition occurs for y^{VS} greater than $\beta_{td}{}^{-1}$ is supported by the measured change in the amount adsorbed, δn, shown in Fig. 5. It is defined by

$$\delta n \equiv \left[\frac{\eta_{td}(1.22) - \eta_{td}(0.95)}{\eta_{td}(0.95)}\right] \tag{44}$$

where 0.95 is the largest value of y^{VS} at which we are able to measure the equilibrium amount adsorbed. The results suggest that the amount adsorbed undergoes a sudden increase to a value that is 57 times larger than the value of η_{td}^{V} at 0.95, and could be characterized as a phase transition.

5.2 The adsorbate entropy indicates a disorder–order phase transition

We now examine the transition for $y^{VS} \geq \beta_{td}{}^{-1}$ from the point of view of the adsorbate entropy. At a given value of y^{VS} for both equilibrium and thermal disequilibrium experiments, the temperature of the solid surface is known, the solid surface area is constant, and the total number of molecules adsorbed is known. For the thermal disequilibrium experiment, the adsorbed phase has been assumed to be in local equilibrium. Thus, we may use the canonical ensemble expression for the entropy of the adsorbate, $s^{SV}(y^{VS})$:

$$s^{SV}(y^{VS}) = -k_B\left[\frac{a_0(y^{VS})}{M}\ln\frac{a_0(y^{VS})}{M} + \sum_{\zeta=1}^{\zeta_m}\frac{a_\zeta(y^{VS})}{M}\ln\frac{a_\zeta(y^{VS})}{M}\right] \tag{45}$$

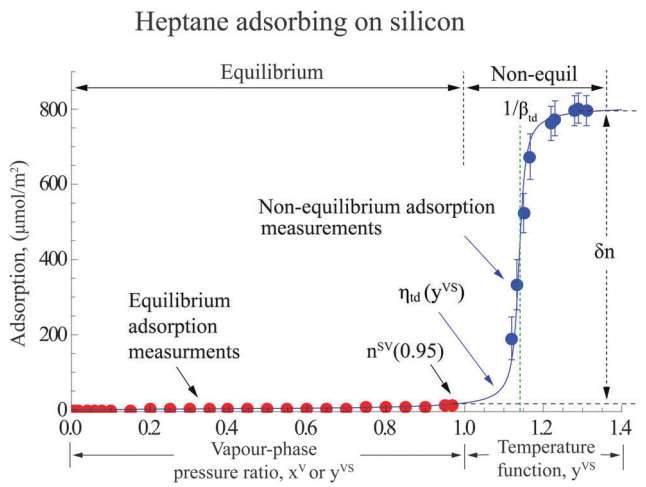

Fig. 5 The adsorption of heptane vapour on silicon is shown for the complete range of y^{VS}. In the phase transition indicated when y^{VS} exceeds $1/\beta_{td}$, the value of δn defined in eqn (44) was 57. The solid line was calculated using eqn (35) with the parameter values listed in Table 2 with ζ_m chosen as 356. Note that there is no measured disagreement between the calculations and either the equilibrium or thermal disequilibrium experiments.

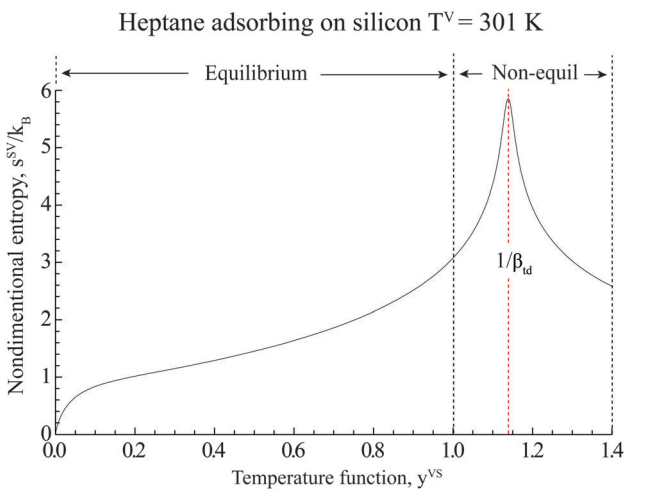

Fig. 6 The non-dimensional entropy of the adsorbate as a function of y^{VS} is shown. At y^{VS} equal to $\beta_{td}{}^{-1}$, the entropy of the adsorbate reaches its maximum value as expected, since the number of clusters of each type, as indicated in Fig. 4 and 7, has the same value, the clusters are identifiable, and thus the quantum mechanical degeneracy of this configuration would be a maximum. As the y^{VS} is increased above $\beta_{td}{}^{-1}$, the entropy of the adsorbate decreases and the adsorbate becomes more ordered.

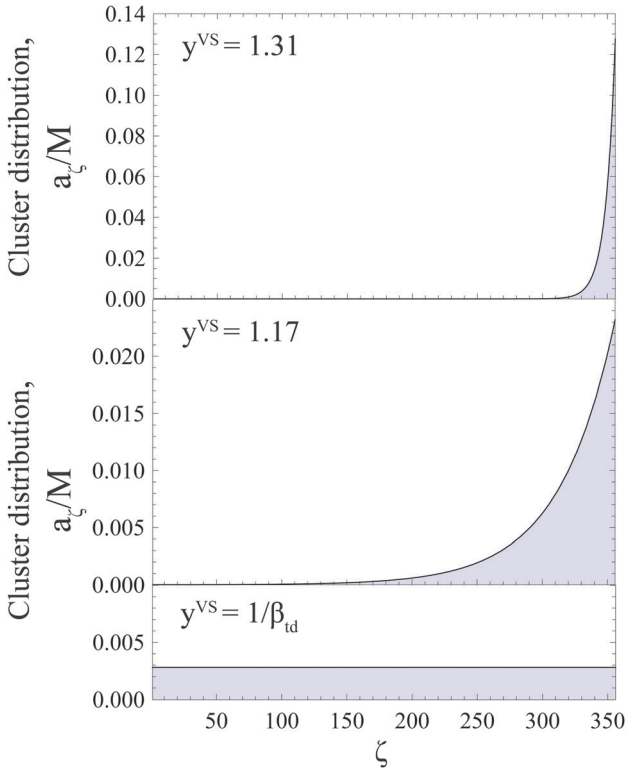

Fig. 7 The number of cluster-types—values of ζ—that are predicted to be present in the adsorbate at three different values of y^{VS} is shown. Their possible concentrations are predicted to be only in the shaded areas. The predictions are that at y^{VS} equal to $1/\beta_{td}$, clusters with ζ molecules are equally probable, independent of the value of ζ; thus, the ζ range is $1 \leq \zeta \leq 356$, and at this value of y^{VS}, the adsorbate is not a film. But as y^{VS} is increased above $1/\beta_{td}$ the range of cluster sizes becomes limited. So that at y^{VS} equal to 1.31, the ζ range is limited to $310 \leq \zeta \leq 356$, and the adsorbate is a well defined film, *e.g.* τ_m is 117 nm ± 4%, Table 1.

where $a_\zeta(y^{VS})/M$ (eqn (33) and (34)) is taken to be the probability of an adsorption site being occupied by a type-ζ cluster and k_B is the Boltzmann constant. Using eqn (33) and (34) and the parameter values listed in Table 2, a plot of s^{SV} as a function of y^{VS} is shown in Fig. 6. At y^{VS} equal to ${\beta_{td}}^{-1}$, the entropy of the adsorbate is seen to have its maximum value.

The reason for the maximum at this value of y^{VS} can be understood from Fig. 7: under this condition, the number of clusters in the adsorbate of each type is the same. Thus, the disorder of the adsorbate would be a maximum because the number of possible adsorbate configurations would also be a maximum.

The decrease in the entropy when y^{VS} is greater than ${\beta_{td}}^{-1}$, seen in Fig. 5, can also be understood from a disorder–order point of view. For the y^{VS} in this range, Fig. 4 and 6 indicate that although the number of clusters is M—no empty sites—and is independent of y^{VS}, the number of cluster-types in the adsorbate is reduced as y^{VS} is increased, as indicated in Fig. 7: when y^{VS} is equal to ${\beta_{td}}^{-1}$ or 1.143, there are predicted to be 356 cluster-types in the adsorbate, and the concentration of molecular cluster of all types is the same: a_ζ/M is equal to 0.003 for all $\zeta \geq$ unity. But when y^{VS} is increased to 1.17, the number of cluster-types is predicted to be reduced: only clusters with more than 100 molecules are predicted to be present in the adsorbate; thus the number of possible cluster-types is 356 minus 100 or 256 cluster-types in the adsorbate (see Fig. 7). When y^{VS} is increased to 1.31, only cluster-types with more than 300 molecules are predicted to be present, or 56 cluster types. As the number of cluster-types is decreased—by reducing T^S relative to T^V—the configurational degeneracy of the adsorbate is predicted to decrease, and therefore so would its entropy or the possible disorder of the adsorbate, as seen in Fig. 6.

The phase transition that is initiated at $y^{VS} \cong {\beta_{td}}^{-1}$ (Fig. 5) is indicated in Fig. 6 and 7 to be the disorder–order phase transition that takes place when thermal disequilibrium exists between the vapour and the adsorbate. From the known value of y^{VS} required to initiate the phase transition, the temperature of the substrate, T^S_β, can be calculated from eqn (7), and is found to be 298.3 ± 0.2 K. Since the temperature of the vapour in these experiments was 301 ± 0.2, we find that the subcooling temperature required to initiate the transition from an adsorbed vapour to adsorbed liquid is 2.7 ± 0.4 K. This result is in contrast to the assumption of the continuum model[1] which assumes that no subcooling is required for the phase change.

6 Discussion

The continuum approach to predicting the thickness of the film formed on a vertically oriented surface in a gravity field when a saturated vapour at $T_{sat}(P^V)$ is in contact with a solid surface that is maintained at a T^S that is less than $T_{sat}(P^V)$ was originally presented by Nusselt[1] in 1916 and his model is still often discussed—over 1100 citations listed on the Web of Science™—but we have not found any experimental confirmation of the Nusselt-based calculations.

The conditions in our experiments correspond closely to those assumed in the Nusselt model: a liquid film lies on the bottom surface of the experimental chamber during our experiments, Fig. 1, and the temperature, T^V, was measured near the liquid–vapour interface. We take the vapour phase to be saturated at this measured temperature. The solid surface temperature, T^S, was determined using the 12 thermocouples that were implanted in the solid substrate.[5] The value of T^S in each experiment is listed in Table 1. In both the Nusselt model and in the approach presented herein, a steady state is assumed to exist in the system.

Both the value of the ΔT, eqn (1), in each of our experiments and the corresponding value of the film thickness calculated from the Nusselt model, δ_c, are listed in Table 1, along with the measured values of the film thickness, τ_m.

Note that in each experiment, the value of δ_c is at least three orders of magnitude greater than that measured. Such a large difference between measurements and model calculations often indicates the difference in conception: in the Nusselt approach the liquid film is assumed to form without the need for subcooling, and the film growth is assumed to be controlled

by thermal energy transport. The expression for this transport was developed using the heat transfer coefficient hypothesis. The vapour was assumed to be stagnant. This reduced the heat transfer problem to a thermal conduction problem.[18] Thermal equilibrium was assumed at both the liquid–vapour and solid–liquid interfaces.

Although assuming the thermal equilibrium at an interface when a phase change is occurring there has been the standard assumption, it has been challenged recently both experimentally[19–22] and by simulations.[4,6] We note that in the cluster approach, it was unnecessary to introduce the heat transfer coefficient or to assume thermal equilibrium at an interface where the phase change was occurring.

In the proposed approach, the basic assumptions were that for a steady state to exist the cluster distributions had to be such that eqn (3) and (6) were satisfied. These assumptions led to an expression for the amount adsorbed, $\eta_{td}(y^{VS})$. As seen in Fig. 5, it was shown to be in agreement with the measured amount adsorbed under both equilibrium and thermal disequilibrium conditions.

7 Conclusion

The molecular cluster approach that was used to develop the Zeta adsorption isotherm for equilibrium vapour adsorption has been extended to calculate the amount of vapour adsorbed under thermal disequilibrium conditions, $\eta_{td}(y^{VS})$. This approach indicates that when heptane vapour at T^V is exposed to a smooth silicon substrate at a T^S that is less than T^V, a steady state cluster distribution forms in which the adsorbate consists of molecular clusters with ζ molecules in each cluster, where ζ can be 1, 2, 3…ζ_m. If thermal equilibrium exists in the system, $\eta_{td}(y^{VS})$ reduces to the equilibrium Zeta adsorption isotherm, $n^{SV}(x^V)$. As a result, as indicated in Fig. 4, $\eta_{td}(y^{VS})$ can be used to calculate the amount adsorbed under both thermal equilibrium and thermal disequilibrium conditions.

Under thermal disequilibrium conditions, when the temperature function, y^{VS}, is increased above unity to $(\beta_{td})^{-1}$, by lowering T^S relative to T^V, a state of maximum disorder is reached in which the number of clusters of each type has the same concentration in the adsorbate, see Fig. 6 and 7. A further increase in the temperature function y^{VS} is predicted to initiate an adsorbed liquid phase by a disorder–order transition, Fig. 5. The adsorbed phase then becomes progressively more uniform as the dispersion in the cluster distribution is reduced as y^{VS} is increased further.

The continuum predictions of the thickness of an adsorbed liquid film as a function of ΔT are remarkably different from those measured using the UV-vis interferometer. The measured film thickness is in agreement with the predictions of the cluster approach, $\eta_{td}(y^{VS})$ as seen in Fig. 4. This difference reflects the difference in the theoretical basis for the predictions. The continuum approach assumes that the liquid phase is initiated whenever ΔT is greater than zero, but the molecular cluster approach indicates that the adsorbed vapour does not make a transition to an adsorbed liquid until ΔT reached 2.7 K or y^{VS} reached 1.143.

Acknowledgements

The authors gratefully acknowledge the support of the Natural Sciences and Engineering Research Council of Canada, Schlumberger Canada Ltd and the Canadian and the European Space Agencies.

References

1 W. Nusselt, *Z. Ver. Dtsch. Ing.*, 1916, **B60**, 541–546.
2 A. Fagri and Y. Zhang, *Transport phenomena in miltiphase systems*, Elesvier, 2006.
3 C. A. Ward and J. Wu, *J. Phys. Chem. B*, 2007, **111**, 3685–3694.
4 R. Hołyst, M. Litniewski, D. Jakubczyk and K. Kolwas, *et al.*, *Rep. Prog. Phys.*, 2013, **76**, 034601.
5 H. Ghasemi and C. A. Ward, *J. Phys. Chem. C*, 2011, **115**, 21311–21319.
6 D. Niu and G. H. Tang, *Sci. Rep.*, 2016, **6**, 19192–19198.
7 J. P. Sethna, *Entropy, Order Parameters, and Complexity*, Clarendon Press, Oxford, U.K., 2011.
8 L. Dufour and R. Defay, *Thermodyhanics of clouds*, Academic Press, 1963.
9 J. Wu, T. Farouk and C. A. Ward, *J. Phys. Chem. B*, 2007, **111**, 6189–6197.
10 H. Ghasemi and C. A. Ward, *J. Phys. Chem. B*, 2009, **113**, 12632–12634.
11 H. Ghasemi and C. A. Ward, *J. Phys. Chem. C*, 2010, **114**, 5088–5100.
12 H. Zandavi and C. A. Ward, *J. Colloid Interface Sci.*, 2013, **407**, 255–264.
13 S. H. Zandavi and C. A. Ward, *Phys. Chem. Chem. Phys.*, 2014, **16**, 10979–10989.
14 S. H. Zandavi and C. A. Ward, *Phys. Chem. Chem. Phys.*, 2015, **17**, 9828–9834.
15 S. H. Zandavi and C. A. Ward, *Energy Fuels*, 2015, **29**, 3004–3010.
16 Y.-J. Hung, S.-L. Lee and L. A. Coldren, *Opt. Express*, 2010, **18**, 6841–6852.
17 Y.-J. Hung, S.-L. Lee, K.-C. Wu, Y. Tai and Y.-T. Pan, *Opt. Express*, 2011, **19**, 15792–15802.
18 L. Landau and E. M. Lifschitz, *Fluid mechanics*, Pergamon Press Ltd, London, 2nd edn, 1987.
19 G. Fang and C. A. Ward, *Phys. Rev. E: Stat. Phys., Plasmas, Fluids, Relat. Interdiscip. Top.*, 1999, **59**, 417–428.
20 F. Duan, C. A. Ward, V. K. Badam and F. Durst, *Phys. Rev. E: Stat., Nonlinear, Soft Matter Phys.*, 2008, **78**, 041130.
21 A. H. Persad and C. A. Ward, *J. Phys. Chem. B*, 2010, **114**, 6107–6116.
22 C. A. Ward and D. Stanga, *Phys. Rev. E: Stat., Nonlinear, Soft Matter Phys.*, 2001, **64**, 051509.

